Delft University of Technology

Delft Center for Systems and Control

Technical report 23-009

Optimal control of offshore wind farm collector systems during outages*

M. Ubbens and B. De Schutter

If you want to cite this report, please use the following reference instead:

M. Ubbens and B. De Schutter, "Optimal control of offshore wind farm collector systems during outages," *Proceedings of the 2023 IEEE International Conference on Communications, Control, and Computing Technologies for Smart Grids (SmartGridComm)*, Glasgow, UK, 6 pp., Oct.–Nov. 2023. doi:10.1109/SmartGridComm57358.2023.10333942

Delft Center for Systems and Control
Delft University of Technology
Mekelweg 2, 2628 CD Delft
The Netherlands
phone: +31-15-278.24.73 (secretary)
URL: https://www.dcsc.tudelft.nl

*This report can also be downloaded via https://pub.bartdeschutter.org/abs/23_009.html

Optimal control of offshore wind farm collector systems during outages

Martiene Ubbens
Business Area Wind
Vattenfall
Amsterdam, The Netherlands
martiene.ubbens@vattenfall.com

Bart De Schutter
Delft Center for Systems and Control
Delft University of Technology
Delft, The Netherlands
b.deschutter@tudelft.nl

***Abstract*—Two optimization-based approaches are proposed to optimize the power routing and turbine setpoints of offshore wind farm (OWF) collector systems during cable outages. The open-loop control strategy assumes that the network can only be reconfigured at the beginning of the outage. In contrast, the receding horizon control strategy is deployed in real time, leveraging cable temperature measurements and power forecasts to derive optimal control actions dynamically. Simulation results concerning occurred outages at an existing OWF prove the practical applicability of the novel approaches and show that both strategies outperform existing approaches.**

***Index Terms*—offshore wind farm operation, collector system outages, optimization-based control, dynamic thermal rating**

I. Introduction

Ambitions to limit climate change are incentivizing the development of renewable energy technologies. One of the most rapidly growing energy markets is offshore wind power. In 2021, its global installed capacity reached 65 GW. In line with the Paris Agreement [1], a UN Global Compact has been signed to commit to the target of 380 GW capacity by 2030 and 2000 GW by 2050 [2]. To meet these ambitious targets, it is vital that the investment costs for Offshore Wind Farms (OWFs) are reduced, and wind power efficiency is increased.

The electrical system of OWFs presents significant potential in this regard. It typically consists of an AC collector system, an example of which is shown in Figure 1, and an export system. Within the collector system, inter-array cables transport the power produced by the turbines to the Offshore Substation (OSS). From the OSS, export cables transport the power to shore. Not only does the electrical system constitute a large portion of the capital expenditure, but its cable outages also account for 80% of the financial losses in the offshore wind industry. For example, the failure of one inter-array cable can cost up to €3 million, depending on the type and location of the failure [3]. These costs are built up of repair costs and costs related to the curtailment of power throughout the outage.

To limit the production losses due to inter-array outages, rerouting can be performed to transport the power produced by the turbines connected to the inoperative cable to the OSS. If the power is rerouted, an elongated string is formed, and turbine setpoints need to be adjusted to prevent overloading of the cables. These setpoints upper-bound the turbine production.

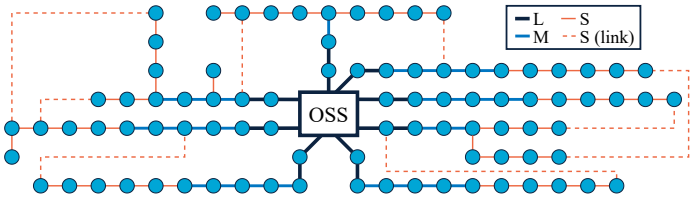

Fig. 1. Schematic of a meshed collector system. The circles represent the turbines. The cable sizes are indicated in the legend. Links are not used during standard operation but are not fundamentally different from the other cables.

In the industry and in [4], a single cable is activated to reroute the power. The authors of [5] develop an optimization-based approach that instead considers the full freedom of the network to distribute the power more evenly over the network. However, their method cannot be used to derive setpoints since it simply assumes that during an outage, curtailment is performed such that the power flow limits are not violated. Like the other mentioned approaches, Static Thermal Rating (STR) is used to constrain the power flows through the network. This rating dictates the maximum amount of power that can flow through the cable continuously. When applied to OWFs, this leads to under-utilization of the network as the fluctuations in wind power are disregarded [6].

Given that inter-array outages typically last more than a month [7], optimizing the rerouting and setpoints can significantly reduce the losses during outages. Moreover, an optimization approach can support the current trend of designing OWFs that are tailored to the site's specifics [8] and OWFs with a larger installed wind power capacity than can be transported via the collector system [6]. Any increase in effectiveness can benefit the entire generating capacity and can aid in realizing the ambitious growth in OWFs targeted.

This work presents two novel control strategies that aim to maximize power production during outages: the open-loop control strategy (Section III) and the receding horizon control strategy (Section IV). The developed control strategies, as well as the approaches taken in the industry and in [4], are applied to a case study (Section V) concerning outages that actually occurred. It is shown that both control strategies outperform the existing approaches in terms of power production.

II. Preliminaries

A. Cable rating

Collector system cables are limited in their capacity by their conductor temperature, which should not exceed 90 °C [9]. Typically, the cables are designed and operated according to their STR. This entails constraining the power flows by the maximum current that can be transported continuously without violating the temperature limit [10]. The calculations used to determine the STR are straightforward but do not consider the thermal time constant of the cables. Given the variability in wind power, this leads to under-utilization of the cables.

The full potential of the cables' capacity can be harvested by dynamically determining the rating based on the cable temperature measured by sensors and predicted by a dynamic temperature model. The authors of [11] use load-based Dynamic Thermal Rating (DTR) to estimate the 6-hour ahead risk of exceeding the temperature limit of an export cable and apply STR for one hour if a risk is identified. For optimal control of collector systems during outages, it might be more suitable to directly incorporate the cable temperature dynamics in the optimization formulation. To this end, a dynamic temperature model fit for optimization must be used, such as the third-order state space model derived in [12]. Its input is the squared current. The parameters are to be found by fitting the model to temperature and loading data.

B. Turbine power production

The rated power of turbine i, P_i^{r}, dictates the maximum power that the turbine can produce. The power that turbine i can generate when operating at full performance is called the possible power, P_i^{poss}. It can be approximated with the turbine's warranted power curve, which is a function of the wind speed. More accurate estimations can be obtained by applying the operational power curve to nacelle wind speed measurements [13].

A setpoint can be applied to limit the power output of a turbine. The actual power output of the turbine is then given by the minimum of the possible power, P_i^{poss}, and the setpoint, P_i^{sp} [4].

C. Power flow

Linear or AC power flow can be used to describe the power flows through the network. Although the linear power flow model is less accurate than the AC power flow model, findings suggest that the severity of the approximation error might be limited for collector systems [4], [5], [14]. In addition, the linearity of the linear power flow method makes it less computationally expensive to use within an optimization framework than the nonlinear AC power flow model. In line with this, most approaches in the literature regarding OWF collector system design optimization use linear power flow since it makes the problems tractable [15]. However, the authors recommend further research to assess the accuracy of the linear power flow formulation for OWF collector systems.

D. Existing control strategies

The method used by the industry performs rerouting via one cable and considers STR to determine the turbine setpoints. The capacity of the most limiting cable in the elongated string is then divided equally over the turbines connected to it.

The authors of [4] extend this approach by considering wind speed measurements to derive setpoints dynamically. The strategy assumes a uniform wind speed within the farm. The warranted power curve is used to transform the park's mean wind speed into possible power. All turbines in the elongated string are provided with this value as a setpoint. Iteratively, new setpoints are calculated based on the violation of the STR if the elongated string is formed. Starting with the turbine that has the largest distance to the OSS, it is determined if an even lower setpoint would eliminate the overload. If so, this setpoint is applied. If not, the turbine is curtailed entirely, and the next turbine in the elongated string is considered. As such, power is transmitted over the shortest distance, minimizing losses.

III. Open-loop control strategy

If there is no automated control system in place, service technicians have to go to the relevant turbines when weather conditions allow it to perform manual switching. In addition, the wind farm operator separately has to log onto each affected turbine to provide a new setpoint. For such an OWF, applying control actions dynamically is inconvenient and costly. To this end, the open-loop control strategy aims to maximize power production during an outage under the constraint that setpoint adaptation and network reconfiguration can only be performed at the beginning of an outage. Due to the long duration of an outage and the uncertainties related to wind power production, STR is applied rather than DTR.

To incorporate the wind power variability into the optimization framework, a probabilistic approach is taken, in which the objective is to maximize the production over a set of scenarios:

$$\max \quad \sum_{s\in\mathcal{S}} \sum_{i\in\mathcal{V}\backslash\{0\}} P_{i,s}\mathbb{P}_s \tag{1}$$

where $\mathcal{V} = \{0, ..., N\}$ denotes the set of nodes pertaining to the OSS and the turbines. Here, N is the number of turbines, and node 0 corresponds to the OSS. The set $\mathcal{S}$ denotes the set of possible power production scenarios, with for each scenario s a probability $\mathbb{P}_s$ and a possible power production $P_{i,s}^{\mathrm{poss}}$. The scenarios can be generated from historical possible power data. The power output of turbine i at scenario s, $P_{i,s}$, is then upper-bounded by the setpoint and the possible power production at that scenario:

$$0 \leq P_{i,s} \leq P_s^{\mathrm{poss}} \qquad \text{for } i \in \mathcal{V}\backslash\{0\},\ s \in \mathcal{S} \tag{2}$$

$$P_{i,s} \leq P_i^{\mathrm{sp}} \qquad \text{for } i \in \mathcal{V}\backslash\{0\},\ s \in \mathcal{S} \tag{3}$$

The resulting control actions are optimal if the set of scenarios is representative of the possible power during the outages.

The STR must not be violated when the turbines are producing at setpoint. Moreover, the applied setpoints must ensure that the STR is also adhered to for any power production conforming to these setpoints. To ensure this under

the uncertainty of the power production over the outage, the network should be operated radially, i.e., a maximum of one outgoing power flow per turbine must be enforced. To this end, a set of arcs, $\mathcal{A}$, is used to describe the operable cables in the network. The cable connecting node i and node j occurs twice within the set of arcs, as (i,j) and (j,i). The radiality constraint can then be captured by the following equations [16]:

$$\sum_{j|(i,j)\in\mathcal{A}} z_{ij} \leq 1 \qquad \text{for } i \in \mathcal{V}\backslash\{0\} \tag{4}$$

$$z_{ij} \in \{0,1\} \qquad \text{for } (i,j) \in \mathcal{A} \tag{5}$$

$$z_{ij} + z_{ji} \leq 1 \qquad \text{for } (i,j) \in \mathcal{A} \tag{6}$$

where the binary variable z_{ij} models the on/off status of cable (i,j). Here, $z_{ij} = 1$ if cable (i,j) can be used and $z_{ij} = 0$ if the cable cannot be used. Equation (6) dictates that power can flow over the same cable in one direction only.

Since radial operation guarantees that the power flows during the outage will never exceed the power flows present when producing at setpoint, the power flow constraints only need to be formulated for the production at setpoint. Furthermore, in the case of radial operation, the linear power flow model can be simplified [5]:

$$0 \leq p_{ij}^{\text{sp}} \leq p_{ij}^{\text{STR}} z_{ij} \qquad \text{for } (i,j) \in \mathcal{A} \tag{7}$$

$$P_i^{\text{sp}} - \sum_{j|(i,j)\in\mathcal{A}} p_{ij}^{\text{sp}} + \sum_{i|(j,i)\in\mathcal{A}} p_{ji}^{\text{sp}} = 0 \qquad \text{for } i \in \mathcal{V} \tag{8}$$

where p_{ij}^{sp} denotes the power flow from node i to node j when all turbines are producing at setpoint and p_{ij}^{STR} is the static thermal rating of cable (i,j).

To prevent switching actions that result in little or no improvement in expected power production, a penalty term can be added to the objective function:

$$\max \quad \left(\sum_{s\in\mathcal{S}} \sum_{i\in\mathcal{V}\backslash\{0\}} P_{i,s}\mathbb{P}_s \right) - c \cdot \sum_{(i,j)\in\mathcal{A}} \zeta_{ij} \tag{9}$$

$$\text{s.t.} \quad -\zeta_{ij} \leq z_{ij} - z_{ij}^{\text{standard}} \leq \zeta_{ij} \quad \text{for } (i,j) \in \mathcal{A} \tag{10}$$

where c is the penalty coefficient, z_{ij}^{standard} is the configuration of the cable under standard operation, and ζ_{ij} is an auxiliary variable enables preservation of the linearity of the objective function. The result is a mixed-integer linear programming (MILP) problem, which can be solved using a brand-and-bound algorithm [17].

IV. Receding Horizon Control Strategy

The receding horizon control strategy assumes that an automated control system is in place that can directly apply setpoint adaptation and network reconfiguration at any given time during the outage. By performing online calculations, cable temperature measurements and power forecasts can be taken into account to tailor the control actions to the specifics of the time step. This allows for constraining the power flows based on the cable temperature limits rather than on the STR.

The control strategy consists of solving two optimization problems at each hour. The first stage is a mixed-integer quadratically constrained programming (MIQCP) problem that finds optimal turbine productions and network topologies over a moving horizon. In this problem, it is assumed that the power forecast is perfect. The second stage then deals with uncertainty in the forecast to prevent unnecessary curtailment if the forecast is too low. The corresponding quadratically constrained linear programming (QCLP) problem aims at finding optimal setpoints for the current hour. While the problems could be merged into one, they are kept separate for clarity.

A radiality constraint as in (4) is no longer posed on the network since taking into account forecasts will allow calculating more precisely how the power will flow through any loops in the network. Deviations from the estimation will not propagate since these will be reflected in the temperature measurements. Therefore, a different set, $\mathcal{E}$, is used to describe the cables than for the open-loop control strategy. In this set of edges, the cable connecting node i and node j occurs only once, limiting the number of binary variables.

A. Stage 1: network reconfiguration

At each hour t, the first stage aims to find optimal network configurations over a prediction window $\mathcal{K}_t = \{t, t+1, ..., t+N_{\text{p}}-1\}$, where N_{p} is the prediction window length. The time interval is 1 hour to be able to model the temperature dynamics. The objective function at hour t aims to maximize the expected power production over the prediction window while penalizing switching actions and distributing curtailment with respect to the power forecast evenly over the network, as stated in (11)-(14). In these equations, $P_{i,k}$ is the power production of turbine i at time step k under the assumption of a perfect forecast, $z_{ij,k}$ is the on/off status of cable (i,j) at time step k, $P_{i,k|t}^{\text{forecast}}$ is the power forecast of turbine i made at hour t concerning time step k, c_1 and c_2 are penalty coefficients, and $\zeta_{ij,k}$ and $\psi_{i,j,k}$ are auxiliary variables. Since

$$\max \quad \sum_{k\in\mathcal{K}_t} \left(\sum_{i\in\mathcal{V}\backslash\{0\}} P_{i,k} - c_1 \cdot \sum_{(i,j)\in\mathcal{E}} \zeta_{ij,k} - c_2 \cdot \sum_{i\in\mathcal{V}\backslash\{0\}} \sum_{j\in\mathcal{V}:j>i} \psi_{i,j,k} \right) \tag{11}$$

$$\text{s.t.} \quad -\zeta_{ij,k} \leq z_{ij,k} - z_{ij,k-1} \leq \zeta_{ij,k} \qquad \text{for } (i,j) \in \mathcal{E},\ k \in \mathcal{K}_t \tag{12}$$

$$0 \leq P_{i,k} \leq P_{i,k|t}^{\text{forecast}} \qquad \text{for } i \in \mathcal{V}\backslash\{0\},\ k \in \mathcal{K}_t \tag{13}$$

$$-\psi_{i,j,k} \leq P_{i,k} - P_{i,k|t}^{\text{forecast}} - P_{j,k} + P_{j,k|t}^{\text{forecast}} \leq \psi_{i,j,k} \qquad \text{for } i \in \mathcal{V}\backslash\{0\},\ j \in \mathcal{V}:j>i,\ k \in \mathcal{K}_t \tag{14}$$

stage 1 assumes that the forecast is perfect, the forecast can be treated as the possible power, leading to (13).

The linear power flow model of [18] is used to model the power flows in the system:

$$P_{i,k} - \sum_{j|(i,j)\in\mathcal{E}} p_{ij,k} + \sum_{j|(j,i)\in\mathcal{E}} p_{ji,k} = 0 \quad \text{for } i \in \mathcal{V},\ k \in \mathcal{K}_t \tag{15}$$

$$z_{ij,k} \in \{0,1\} \quad \text{for } (i,j) \in \mathcal{E},\ k \in \mathcal{K}_t \tag{16}$$

$$-M_{ij} z_{ij,k} \leq p_{ij,k} \leq M_{ij} z_{ij,k} \quad \text{for } (i,j) \in \mathcal{E},\ k \in \mathcal{K}_t \tag{17}$$

$$p_{ij,k} \leq b_{ij}(\theta_{i,k} - \theta_{j,k}) + M_{ij}(1 - z_{ij,k}) \quad \text{for } (i,j) \in \mathcal{E},\ k \in \mathcal{K}_t \tag{18}$$

$$p_{ij,k} \geq b_{ij}(\theta_{i,k} - \theta_{j,k}) - M_{ij}(1 - z_{ij,k}) \quad \text{for } (i,j) \in \mathcal{E},\ k \in \mathcal{K}_t \tag{19}$$

where $p_{ij,k}$ is the power flow through cable (i,j) at time step k, b_{ij} is the admittance of cable (i,j), and $\theta_{i,k}$ is the voltage angle of node i at time step k. The latter is defined relative to a reference voltage phasor. This is typically the node pertaining to the OSS, of which the voltage angle is then fixed to zero. The power (flow) and admittance are expressed in per-unit values and the voltage angles in radians. Furthermore, M_{ij} can be selected as $2b_{ij}\theta^{\max}$, in which $\theta^{\max}$ is the maximum voltage angle.

A discretized version of the thermal model of [12] can be used to estimate future cable temperatures:

$$T_{ij,t+1} = a_{ij}T_{ij,t} + b_{ij}T_{ij,t-1} + c_{ij}T_{ij,t-2} + d_{ij}p_{ij,t}^2 + e_{ij} \tag{20}$$

where $T_{ij,t}$ is the temperature of cable (i,j) at hour t, $p_{ij,t}$ is the power flow through cable (i,j) at hour t, and a_{ij}, b_{ij}, c_{ij}, d_{ij}, and e_{ij} are cable and location-specific parameters that can be found by fitting the model to temperature and power data. With respect to the state-space model of [12], the term e_{ij} has been added since this turns out to result in a better fit for the data of the case study of Section V. To predict future cable temperatures, the model must be initialized with three Distributed Temperature Sensing (DTS) measurements, $T_{ij,t}^{\mathrm{DTS}}$, $T_{ij,t-1}^{\mathrm{DTS}}$, and $T_{ij,t-2}^{\mathrm{DTS}}$. For the first two prediction steps, the future temperatures can then be constrained as follows:

$$T_{t+1|t} = aT_t^{\mathrm{DTS}} + bT_{t-1}^{\mathrm{DTS}} + cT_{t-2}^{\mathrm{DTS}} + dp_t^2 + e \leq T^{\max} \tag{21}$$

$$T_{t+2|t} = aT_{t+1|t} + bT_t^{\mathrm{DTS}} + cT_{t-1}^{\mathrm{DTS}} + dp_{t+1}^2 + e = (a^2+b)T_t^{\mathrm{DTS}} + (ab+c)T_{t-1}^{\mathrm{DTS}} + acT_{t-2}^{\mathrm{DTS}} + adp_t^2 + dp_{t+1}^2 + ae + e \leq T^{\max} \tag{22}$$

where $T^{\max}$ is the cable temperature limit and the index ij is dropped for clarity. The power flow constraints can be formulated without explicitly defining the temperatures, which avoids the use of quadratic equality constraints:

$$F_{ij}\begin{bmatrix} T_{ij,t}^{\mathrm{DTS}} \\ T_{ij,t-1}^{\mathrm{DTS}} \\ T_{ij,t-2}^{\mathrm{DTS}} \end{bmatrix} + G_{ij}\begin{bmatrix} p_{ij,t}^2 \\ p_{ij,t+1}^2 \\ \vdots \\ p_{ij,t+N_{\mathrm{p}}-1}^2 \end{bmatrix} + H_{ij} \leq T_{N_{\mathrm{p}}\times 1}^{\max} \quad \text{for } (i,j) \in \mathcal{E} \tag{23}$$

where $F_{ij} \in \mathbb{R}^{N_{\mathrm{p}}\times 3}$, $G_{ij} \in \mathbb{R}^{N_{\mathrm{p}}\times N_{\mathrm{p}}}$, and $H_{ij} \in \mathbb{R}^{N_{\mathrm{p}}\times 1}$ are matrices parameterized by a_{ij}, b_{ij}, c_{ij}, d_{ij}, and e_{ij}. Furthermore, $T_{N_{\mathrm{p}}\times 1}^{\max}$ is a vector of length N_{p}, each element being $T^{\max}$.

At each hour t, the optimization problem of (11)-(19) and (23) is formulated using the measured cable temperatures and the most recent power forecast. The optimal network configuration pertaining to the current hour is applied to the network.

B. Stage 2: setpoint adaptation

The second stage uses $z_{ij,t}$ and $P_{i,t}$ as input to calculate the optimal setpoints for the current hour. Its objective function is to maximize the setpoints while aiming to distribute the deviations of the turbine setpoints from the power forecast evenly over the network. By doing so, the strategy assumes that any inaccuracy in the power forecast affects the turbines to the same extent. The optimization framework is the following:

$$\max \quad \sum_{i\in\mathcal{V}\setminus\{0\}} P_{i,t}^{\mathrm{sp}} - c_3 \cdot \sum_{i\in\mathcal{V}\setminus\{0\}} \sum_{j\in\mathcal{V}:j>i} \varrho_{i,j,t} \tag{24}$$

$$\text{s.t.} \quad -\varrho_{i,j,t} \leq P_{i,t}^{\mathrm{sp}} - P_{i,t|t}^{\mathrm{forecast}} - P_{j,t}^{\mathrm{sp}} + P_{j,t|t}^{\mathrm{forecast}} \leq \varrho_{i,j,t} \quad \text{for } i \in \mathcal{V}\setminus\{0\},\ j \in \mathcal{V} : j > i \tag{25}$$

$$a_{ij}T_{ij,t}^{\mathrm{DTS}} + b_{ij}T_{ij,t-1}^{\mathrm{DTS}} + c_{ij}T_{ij,t-2}^{\mathrm{DTS}} + d_{ij}(p_{ij,t}^{\mathrm{sp}})^2 + e_{ij} \leq T^{\max} \quad \text{for } (i,j) \in \mathcal{E} \tag{26}$$

$$P_{i,t}^{\mathrm{sp}} - \sum_{j|(i,j)\in\mathcal{E}} p_{ij,t}^{\mathrm{sp}} + \sum_{j|(j,i)\in\mathcal{E}} p_{ji,t}^{\mathrm{sp}} = 0 \quad \text{for } i \in \mathcal{V} \tag{27}$$

$$p_{ij,t}^{\mathrm{sp}} = z_{ij,t}b_{ij}(\theta_{i,t}^{\mathrm{sp}} - \theta_{j,t}^{\mathrm{sp}}) \quad \text{for } (i,j) \in \mathcal{E} \tag{28}$$

$$P_{i,t} \leq P_{i,t}^{\mathrm{sp}} \quad \text{for } i \in \mathcal{V}\setminus\{0\} \tag{29}$$

$$0 \leq P_{i,t}^{\mathrm{sp}} \leq P_i^{\mathrm{r}} \quad \text{for } i \in \mathcal{V}\setminus\{0\} \tag{30}$$

In these equations, the variables with the superscript sp denote the previously introduced variables in case of production at setpoint. Furthermore, c_3 is a penalty coefficient, and $\varrho_{i,j,t}$ is an auxiliary variable.

Since for this stage, $z_{ij,t}$ are parameters rather than optimization variables, the linear power flow model introduced in (15)-(19) can be reduced to (28) while preserving linearity. Furthermore, the setpoints must make it possible to produce at least the power production conforming to the power flow limits under the assumption of a perfect forecast, $P_{i,t}$, found in the first stage. This is dictated by (29).

The setpoints found by the second stage are applied to the turbines. The optimization problems of both stages are reformulated at the next iteration using the updated measurements.

V. Case Study

The novel strategies and existing strategies, described in Section II-D, are applied to a case study concerning seven outages that occurred at an existing OWF with a meshed layout. The farm comprises 70 to 100 turbines and contains three distinct cable sizes. Figure 1 shows a fictitious, comparable layout.

A. Data

Possible power, cable temperature, wind speed, and power forecasting data are required to implement the control strategies and to perform simulations. All data is supplied by Vattenfall. Due to confidentiality restrictions, the data cannot be made publicly available.

The possible power is taken to be the maximum of the active power output of the turbine and a possible power signal derived from nacelle wind speed measurements and the operational power curve. The possible power is given per turbine per 10 minutes. Possible power data is also needed to generate the scenarios for the open-loop control strategy. To this end, five years of historical possible power data are binned into groups, for each of which the probability is calculated.

A cable temperature model fitted to cable temperature and power flow data is used to generate synthetic cable temperature measurements during the simulations. With respect to (20), noise terms are added to simulate process and measurement noise:

$$T_{ij,t+1} = a_{ij}T_{ij,t} + b_{ij}T_{ij,t-1} + c_{ij}T_{ij,t-2} + d_{ij}p_{ij,t}^2 + e_{ij} + \varepsilon_{ij,t} \quad (31)$$

$$T_{ij,t}^{\mathrm{DTS}} = T_{ij,t} + \varepsilon_{ij,t} \quad (32)$$

where $\varepsilon_{ij,t}$ is drawn from a zero-mean normal distribution with its variance identified per cable during system identification.

During outages, cables might experience higher power flows than under standard operation. Therefore, per cable size, the cable that experiences the highest power flow is used for identifying a thermal model. The model corresponding to the medium-sized cable is used for the small-sized cables since, during outages, some of the small-sized cables might experience much higher loads than those in the data set.

For parameter estimation, 4.5 months of hourly cable temperature and power flow data are used. 80% of the data is used for system identification, while the final 20% is used for evaluating the quality of the model.

Matlab's function `greyest` [19] is used, which applies nonlinear least squares identification for the problem at hand. The focus is set to simulation instead of prediction, which means that the simulation error is minimized rather than the 1-step ahead prediction error. For the medium- and large-sized cable, the resulting Normalized Mean Square Error (NMSE) fit is 92.8% and 95.8%, respectively. For comparison, note that in [12], a fit of 82.5% to export cable data was reported.

B. Implementation

The novel control strategies are implemented in Python using the modeling framework Pyomo [20] and are solved with Gurobi [21] on a Vattenfall compute cluster (16 vCPU, 256 GiB, AMD EPYC 7452 2.35 GHz processor).

The length N_{p} of the prediction window and the penalty coefficient c_1 of the receding horizon control strategy have been selected based on manual tuning. Here, $N_{\mathrm{p}} = 3$ h and $c_1 = 3$ were the most suited. The remainder of the penalty coefficients are set to $c = 0.01$, $c_2 = 0.001$, and $c_3 = 0.001$.

The strategy of [4], hereafter referred to as the literature control strategy, is derived for OWFs with loop connection cables. For those OWFs, only one cable can be used to reroute the power. The strategy does not consider how to perform rerouting for meshed networks. For the case study, the cable that results in the highest setpoints is activated, similar to the industry strategy. Furthermore, if further reduction in setpoint is not necessary at the measured wind speed, the highest turbine power for which the STR is not violated is applied as setpoint. This approach differs from [4], which applies the power production at measured wind speed as a setpoint. However, for the case study, in which the wind profile is not homogeneous within the farm, that would result in unnecessary curtailment.

In addition, it is calculated what the production would have been if all turbines connected to the inoperative cable were curtailed and no further control actions were taken. This is referred to as the base strategy.

C. Results

For each control strategy and outage, the percentual gap with possible power is listed in Table I. By way of illustration, the power production during outages 2 and 6 is shown in Figure 2 and Figure 3, respectively. As can be seen, the receding horizon control strategy outperforms the other control strategies for all outages. A more elaborate presentation of the outcomes of the case study is given in [22].

The increase in production can mainly be attributed to the use of DTR. Dynamic switching further enables exploiting DTR to the fullest by (de)activating cables during the outage

TABLE I
POWER PRODUCTION RELATIVE TO THE POSSIBLE POWER FOR EACH OUTAGE AND CONTROL STRATEGY.

	Base	Industry	Literature	Open-loop	Receding horizon
1	-8.69%	-5.22%	-6.05%	-5.12%	-2.85%
2	-18.72%	-13.21%	-15.28%	-12.30%	-7.21%
3	-7.13%	-3.57%	-3.68%	-3.55%	-2.42%
4	-6.19%	-4.44%	-4.52%	-4.15%	-1.45%
5	-11.10%	-8.58%	-8.39%	-7.33%	-4.77%
6	-9.75%	-7.62%	-7.57%	-5.74%	-0.36%
7	-9.60%	-5.82%	-5.93%	-4.97%	-2.41%

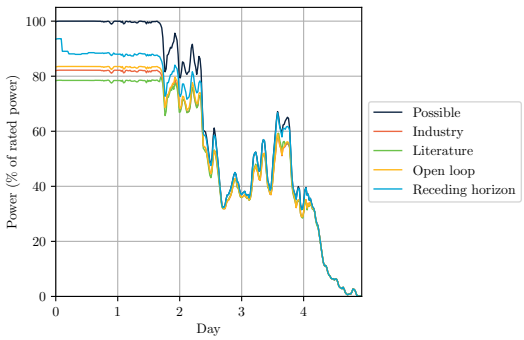

Fig. 2. Power production for outage 2.

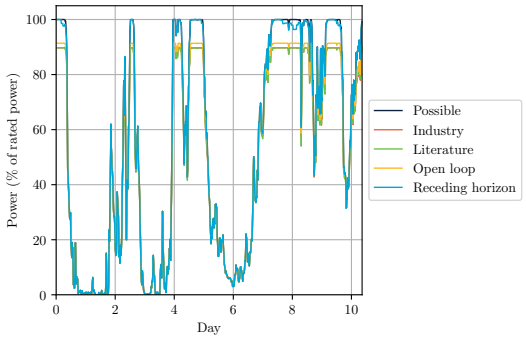

Fig. 3. Power production for outage 6.

based on the cable temperatures and forecasts. The computations for one time step are performed within 23 s on average, with a maximum computation time of 35 minutes.

The open-loop control strategy is a promising alternative if there is no automated control system. This strategy outperforms the industry strategy and the literature strategy in terms of production, with fast computations, i.e., on average 0.34 s.

By using real possible power data that differentiates between turbines, it could be shown that the method in [4] cannot deal well with non-uniform wind speeds within the park and inaccuracies in the warranted power curve.

The average increase in power production with respect to the industry control strategy is 0.82% and 4.2% for the open-loop and receding horizon control strategy, respectively. With an average offshore wind farm size of 301 MW [23], an average capacity factor of 0.42 [23], and an average outage duration of 38 days [7], the estimated increase in power production per outage is 951 MWh for the open-loop and 4.84 GWh for the receding horizon control strategy. With a feed-in remuneration of €194/MWh [4], this translates into a revenue increase per outage of €0.18 million and €0.94 million, respectively.

VI. Conclusions

We have presented two novel optimization-based rerouting and setpoint decision frameworks for outages in OWF collector systems with arbitrary topologies: the open-loop control strategy and the receding horizon control strategy. The performance of these strategies is compared to existing control strategies by simulations with real data from occurred outages. It is shown that both developed strategies outperform the existing control strategies. In particular, the receding horizon control strategy enables a significant decrease in the loss of production during outages.

Future work will focus on incorporating DTR in the operations of collector systems. The thermal model should be fitted per cable to account for location-specific properties instead of using the same parameters per cable size. Ambient conditions can be considered by applying adaptive receding horizon control, in which the temperature model gradually evolves with time. This would allow for considering changing operating conditions without explicitly providing these to the controller.

Acknowledgment

We want to thank Adel Haghani from Vattenfall BA Wind for his valuable feedback and support.

References

[1] UNFCCC, "The Paris Agreement," 2015. UNTC XXVII 7.d.
[2] GWEC, "Global offshore wind report 2022," Tech. rep., Global Wind Energy Council, 2022. https://gwec.net/gwecs-global-offshore-wind-report, accessed December 2022.
[3] E. Gulski, G. J. Anders, R. A. Jongen, J. Parciak, J. Siemiński, E. Piesowicz, S. Paszkiewicz, and I. Irska, "Discussion of electrical and thermal aspects of offshore wind farms' power cables reliability," *Renewable and Sustainable Energy Reviews*, vol. 151, p. 111580, 2021.
[4] J. Scholz, E. Wiebe, V. Scheffer, and C. Becker, "Economic power control for offshore wind farms with loop connection cables," *Automatisierungstechnik*, vol. 68, no. 9, pp. 765–780, 2020.
[5] B. Wang, X. Wang, Z. Song, L. Zhang, S. Wang, and C. Xin, "Fault state operation analysis for offshore wind farm with ring-topology collector system: An OPF and topology optimization method," in *2021 IEEE 5th Conference on Energy Internet and Energy System Integration (EI2)*, pp. 119–124, 2021.
[6] M. A. H. Colin and J. A. Pilgrim, "Cable thermal risk estimation for overplanted wind farms," *IEEE Transactions on Power Delivery*, vol. 35, no. 2, pp. 609–617, 2019.
[7] C. Strang-Moran, "Subsea cable management: Failure trending for offshore wind," *Wind Energy Science Discussions*, pp. 1–11, 2020.
[8] O. Anaya-Lara, "Offshore wind farm arrays," in *Offshore Wind Farms*, pp. 389–417, Elsevier, 2016.
[9] S. Catmull, R. D. Chippendale, J. A. Pilgrim, G. Hutton, and P. Cangy, "Cyclic load profiles for offshore wind farm cable rating," *IEEE Transactions on Power Delivery*, vol. 31, pp. 1242–1250, 2016.
[10] IEC, "IEC 60287-1: Electric cables – calculation of the current rating, Part 1: Current rating equations (100% load factor) and calculation of losses," International standard, International Electrotechnical Organization, 2014.
[11] M. A. H. Colin, J. Dix, and J. A. Pilgrim, "Export cable rating optimisation by wind power ramp and thermal risk estimation," *IET Renewable Power Generation*, vol. 15, pp. 1564–1581, 2021.
[12] S. H. H. Kazmi, *Dynamic Rating Based Design and Operation of Offshore Windfarm Export Systems*. PhD thesis, Technical University of Denmark, 2021.
[13] Y. Wang, Q. Hu, L. Li, A. M. Foley, and D. Srinivasan, "Approaches to wind power curve modeling: A review and discussion," *Renewable and Sustainable Energy Reviews*, vol. 116, p. 109422, 2019.
[14] K. Purchala, L. Meeus, D. Van Dommelen, and R. Belmans, "Usefulness of DC power flow for active power flow analysis," in *IEEE Power Engineering Society General Meeting, 2005*, pp. 454–459 Vol. 1, 2005.
[15] S. Lumbreras, A. Ramos, and P. Sánchez-Martin, "Offshore wind farm electrical design using a hybrid of ordinal optimization and mixed-integer programming," *Wind Energy*, vol. 18, no. 12, pp. 2241–2258, 2015.
[16] M. Fischetti and D. Pisinger, "Optimizing wind farm cable routing considering power losses," *European Journal of Operational Research*, vol. 270, no. 3, pp. 917–930, 2018.
[17] V. Paschos, *Concepts of Combinatorial Optimization*. Wiley, 2014.
[18] E. B. Fisher, R. P. O'Neill, and M. C. Ferris, "Optimal transmission switching," *IEEE Transactions on Power Systems*, vol. 23, no. 3, pp. 1346–1355, 2008.
[19] The MathWorks, Inc., "greyest." https://nl.mathworks.com/help/ident/ref/\greyest.html, accessed May 2023.
[20] M. L. Bynum, G. A. Hackebeil, W. E. Hart, and C. D. Laird, *Pyomo–Optimization Modeling in Python*, vol. 67. Springer Science & Business Media, third ed., 2021.
[21] Gurobi Optimization, LLC, "Gurobi Optimizer Reference Manual," 2023. https://www.gurobi.com.
[22] M. Ubbens, "Optimal control of offshore wind farm collector systems during outages," master's thesis, Delft University of Technology, 2023. Available at http://resolver.tudelft.nl/uuid:8025c9dd-b7c2-4816-9bc2-98e744e5f2b7.
[23] M. Bilgili and H. Alphan, "Global growth in offshore wind turbine technology," *Clean Technologies and Environmental Policy*, vol. 24, no. 7, pp. 2215–2227, 2022.